doi:10.1038/nature09974

Supplementary Figures and Legends

This file contains figures describing the DNA analyses of the Beatrix Au mine mining water filter, the morphology of *Halicephalobus mephisto* sp. n., the phylogenetic trees for the nematode strains, the rarefaction curves and phylogenetic tree for the microbial communities and photomicrographs of the microbial cells.

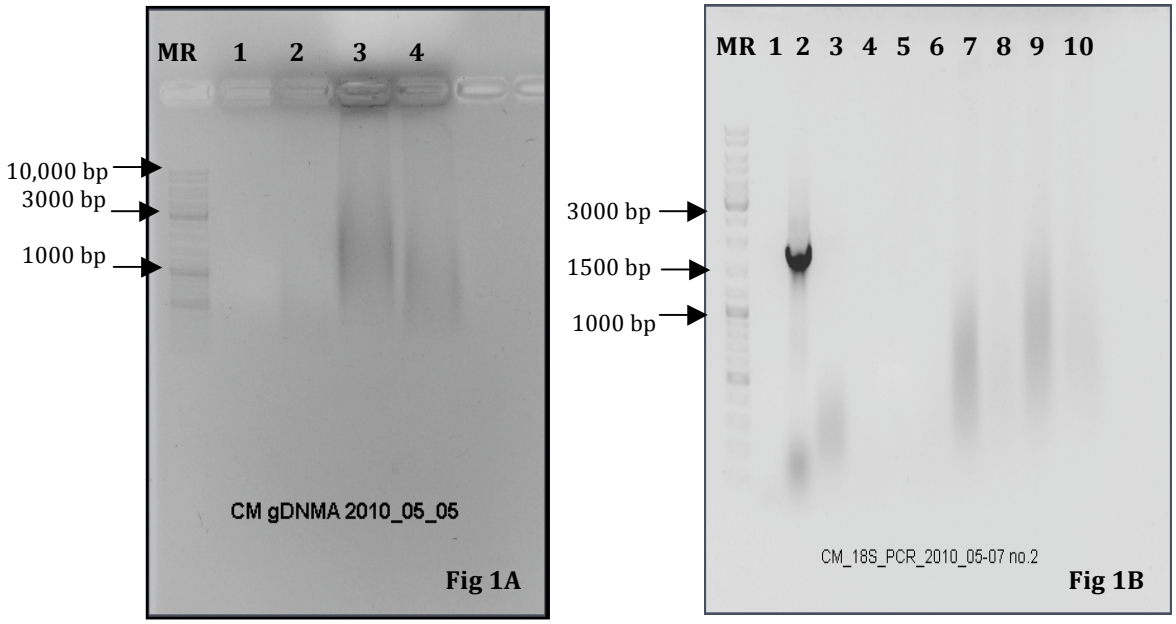

Supplementary Figure 1. A. Genomic DNA isolated from in-line filter. Lane 1: Internal filter layer; Lane 2: External filter layer; Lane 3: Internal net-layer; lane 4: External net-layer. MR represents Generuler^{TM} DNA ladder mix (Fermentas). **B.** The 18S rRNA gene amplification of the isolated DNA. Lane 1: Non-template control; Lane 2: Positive control (*Yarrowia lipolytica*); Lane 3: Internal filter layer spiked with positive control; Lane 4: Internal filter layer; Layer 5: External filter layer spiked with positive control; Lane 6: External filter layer; Lane 7: Internal net-layer spiked with positive control; Lane 8: Internal net layer; Lane 9: External net-layer spiked with positive control; Lane 10: External net-layer.

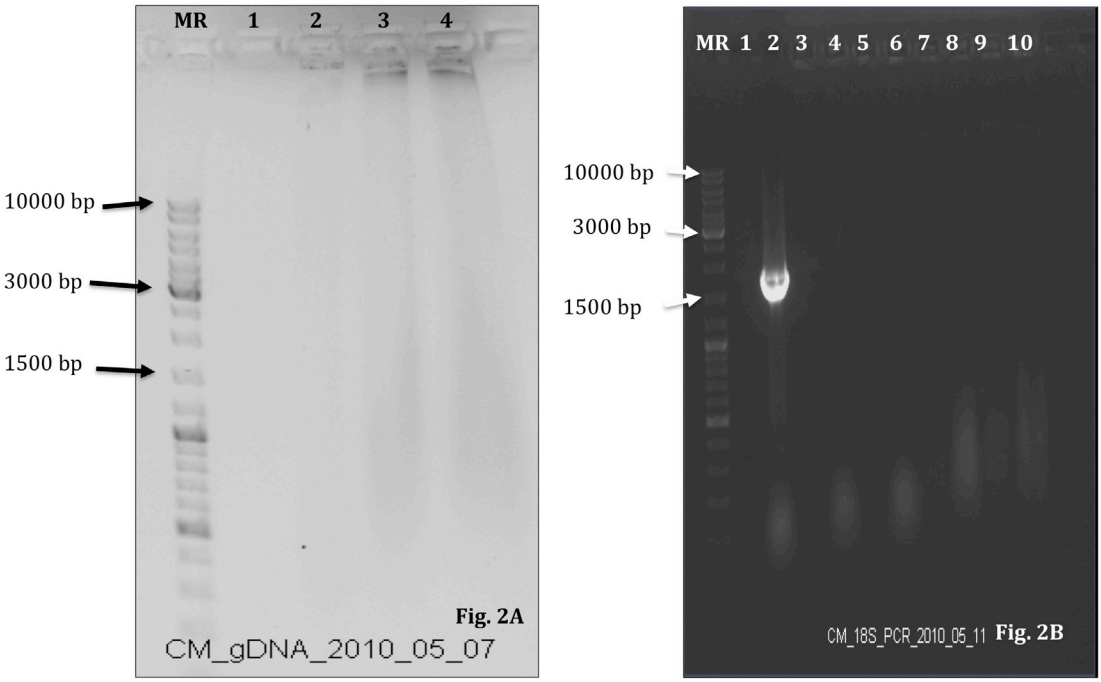

Supplementary Figure 2. **A**. The purified genomic DNA. Lane 1: Internal filter layer; Lane 2: External filter layer; Lane 3: Internal net-layer; lane 4: External net-layer. MR represents Generuler^{TM} DNA ladder mix from Fermentas. **B.** The 18S rRNA gene amplification of the purified DNA. Lane 1: Non-template control; Lane 2: Positive control (*Yarrowia lipolytica*); Lane 3: Internal filter layer spiked with positive control; Lane 4: Internal filter layer; Layer 5: External filter layer spiked with positive control; Lane 6: External filter layer; Lane 7: Internal net-layer spiked with positive control; Lane 8: Internal net layer; Lane 9: External net-layer spiked with positive control; Lane 10: External net-layer.

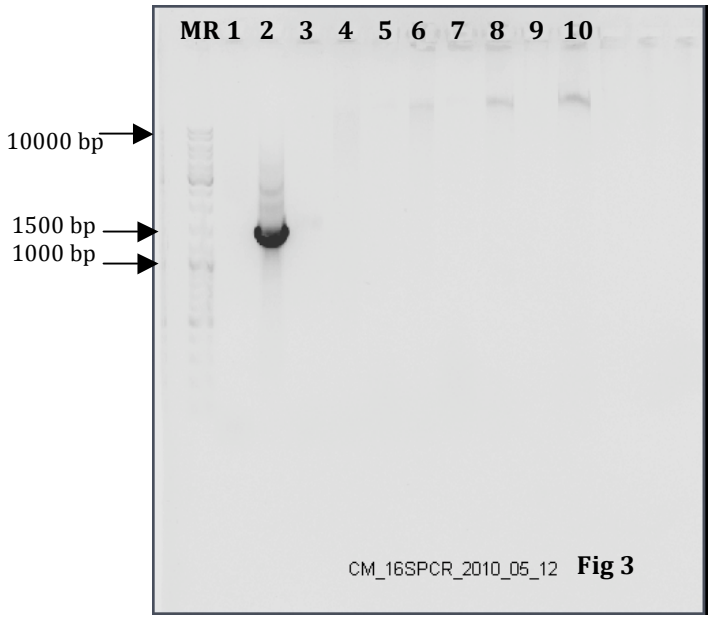

Supplementary Figure 3. The bacterial 16S rRNA amplification of the isolated DNA. Lane 1: Non-template control; Lane 2: Positive control (*Escherichia coli*); Lane 3: Internal filter layer spiked with positive control; Lane 4: Internal filter layer; Layer 5: External filter layer spiked with positive control; Lane 6: External filter layer; Lane 7: Internal net-layer spiked with positive control; Lane 8: Internal net layer; Lane 9: External net-layer spiked with positive control; Lane 10: External net-layer.

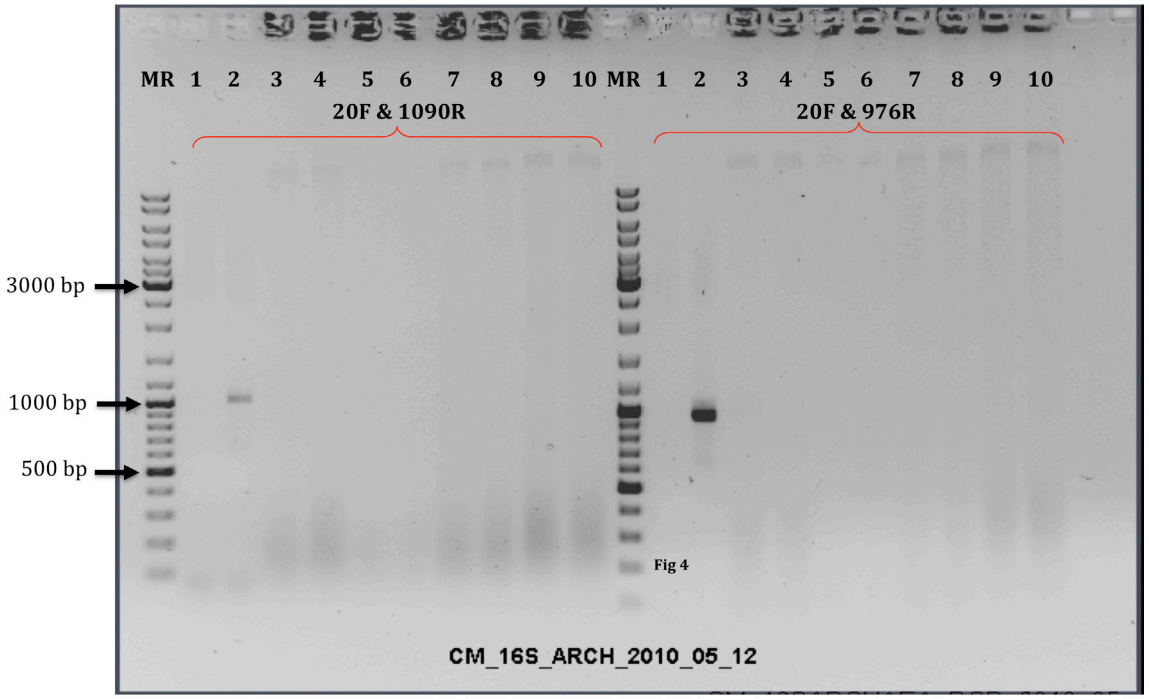

Supplementary Figure 4. The archaeal 16S rRNA gene amplification of the isolated DNA utilizing 20F and 1090R (left) and 20F and 976R (right). Lane 1: Non-template control; Lane 2: Positive control (*Halobacterium salinarum*); Lane 3: Internal filter layer spiked with positive control; Lane 4: Internal filter layer; Layer 5: External filter layer spiked with positive control; Lane 6: External filter layer; Lane 7: Internal net-layer spiked with positive control; Lane 8: Internal net layer; Lane 9: External net-layer spiked with positive control; Lane 10: External net-layer.

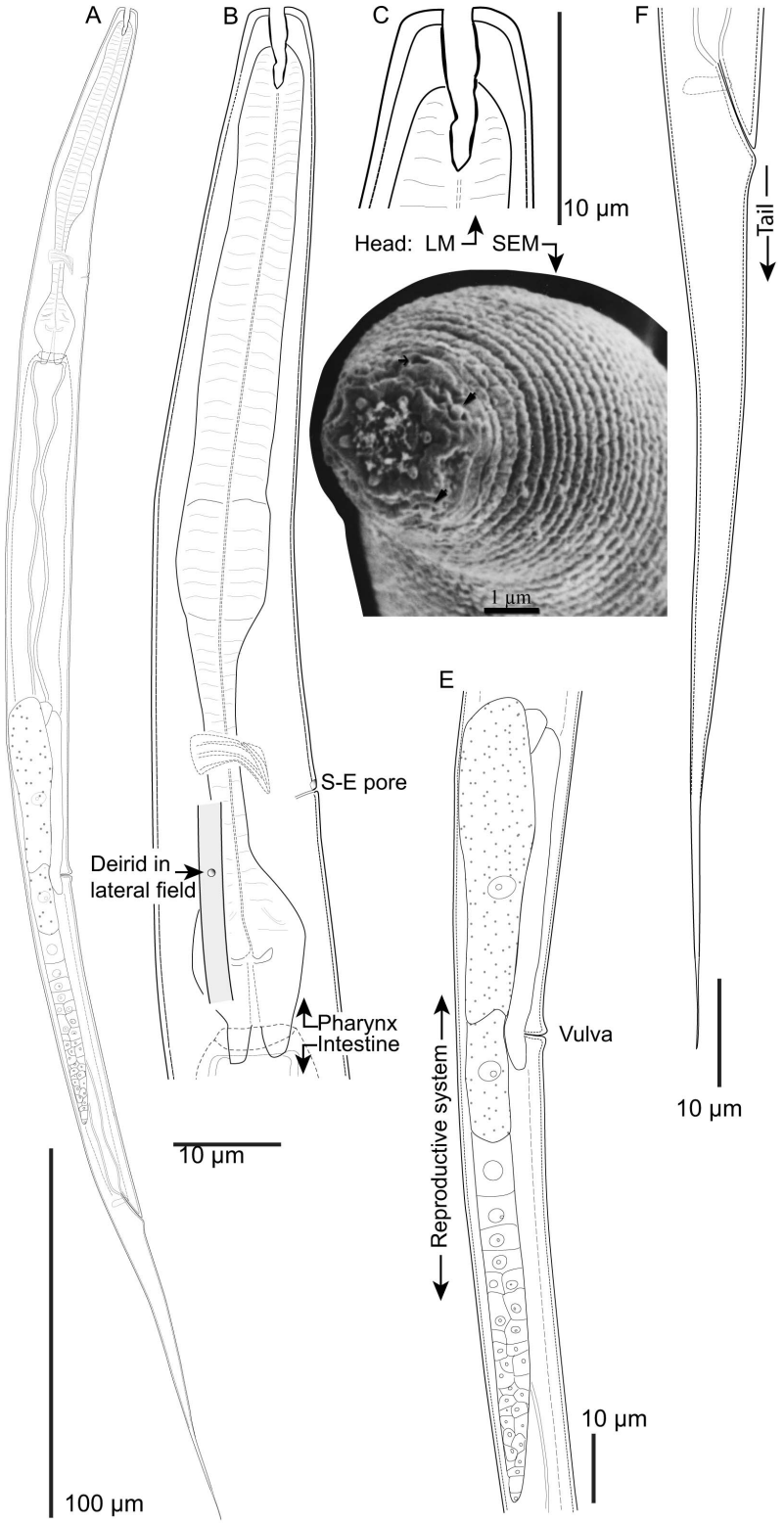

Supplementary Figure 5. General morphology of *Halicephalobus mephisto* n. sp.; LM drawings of female holotype and SEM photograph of head. A: Entire body; B: Neck region; C: anterior region; D: SEM *en face* view; E: reproductive system; F: tail.

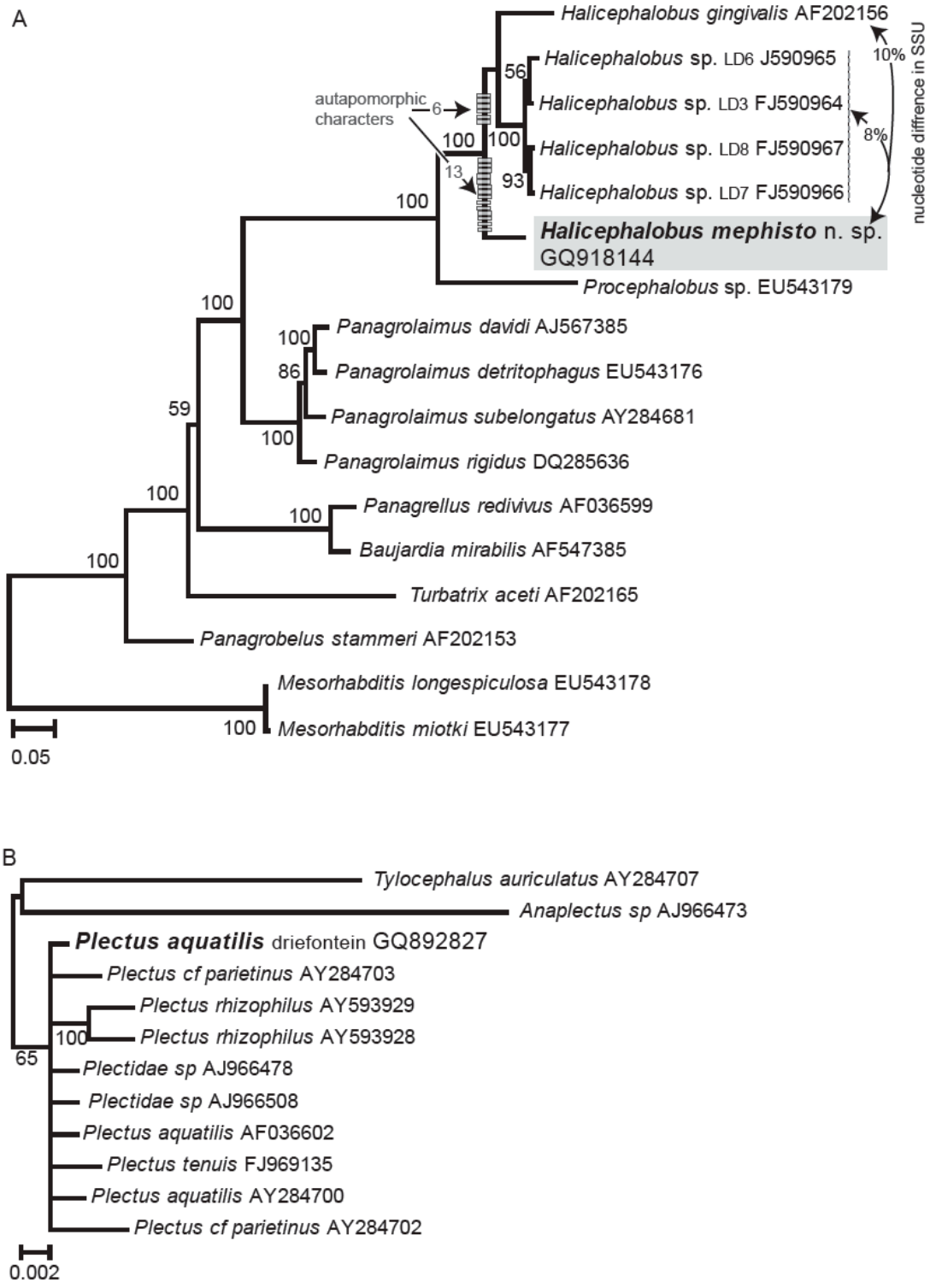

Supplementary Figure 6. Bayesian interference 50% majority rule consensus phylogenies, based on SSU rDNA data, of *Halicephalobus mephisto* (A) and *Plectus aquatilis* (B) analyzed with GenBank sequences of closely related taxa. Branch support is indicated with Posterior Probability values. Scale bar indicates expected substitutions per site.

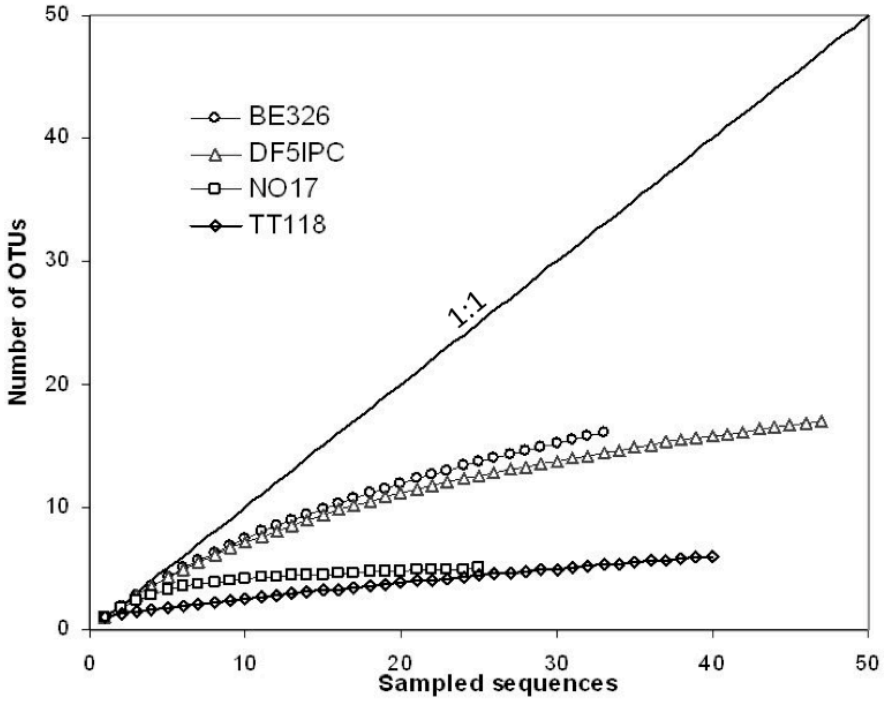

Supplementary Figure 7. The number of OTUs versus the total number of 16S rRNA gene sequences for clone libraries from the Beatrix (BE326), Zondereinde (NO17), Driefontein (DF5IPC) and Tau Tona (TT118) boreholes. Sequences were sorted in OTUs using a 97% identity threshold. The straight line corresponds to a ratio of OTUs to clone number of unity.

Supplementary Figure 8. Neighbour-joining phylogenetic tree chosen as a consensus tree showing the relationship between representative 16S rRNA gene clones from Beatrix (BE326), Zondereinde (NO17), Driefontein (DF5IPC) and Tau Tona (TT118) mines and some related strains and environmental clones from different bacterial and archaeal phyla (GenBank). Accession numbers and number of sequences grouped into that specific OTU are indicated in parentheses. The values of 1,000 bootstrap trial replications are given for nodes with ≥40% support. Taxonomic classification is also shown. The scale bar represents 0.1 nucleotide substitutions per sequence position.

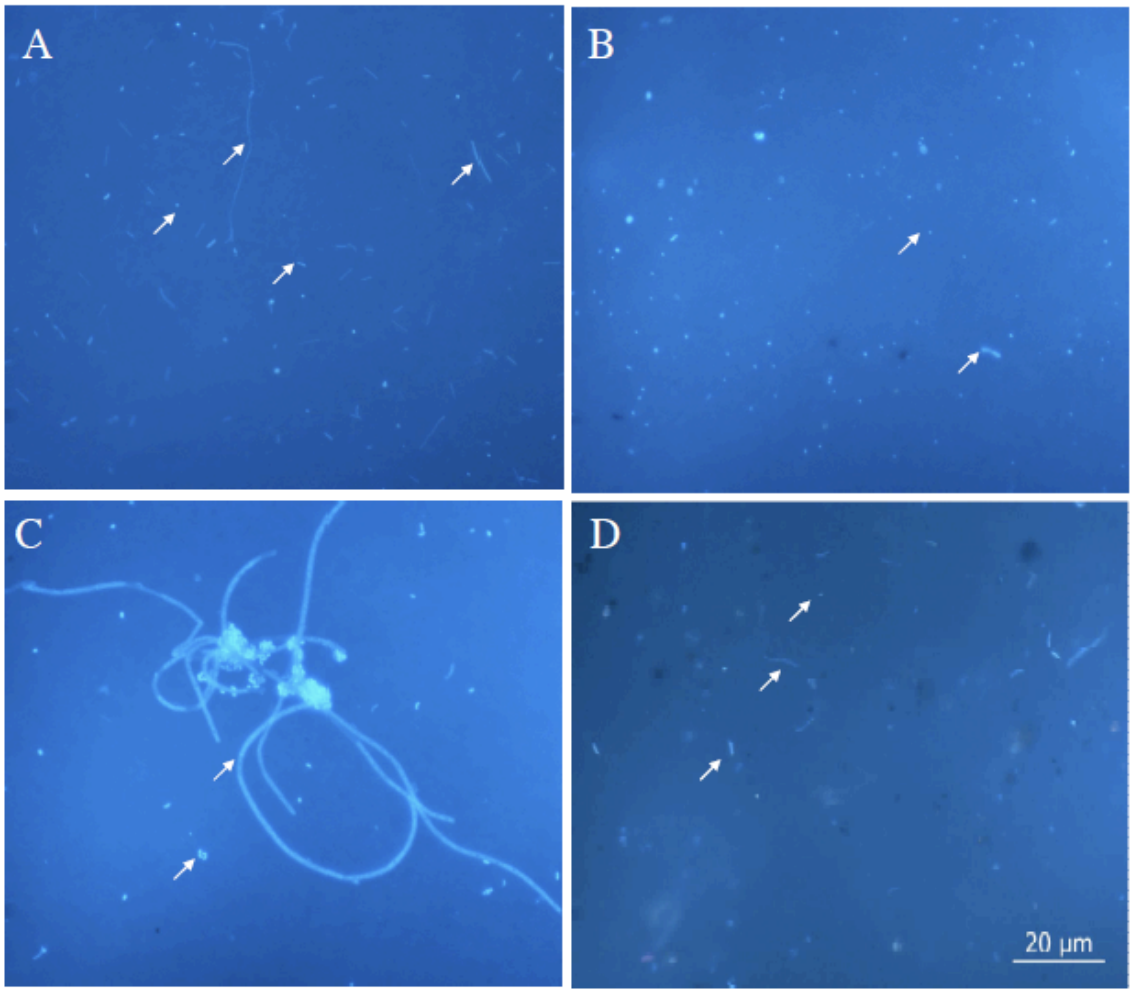

Supplementary Figure 9. Photomicrographs of DAPI-stained cells in samples from A. Beatrix (BE326), B. Zondereinde (NO17), C. Driefontein (DF5IPC) and D. Tau Tona (TT118) borehole water samples, showing the variable morphology (arrows) and cell density. Microbial biomass appeared higher in Beatrix and Tau Tona, which also showed more variable morphotypes (long and short rods, filaments and cocci) compared to Zondereinde (mostly cocci and some short rods) and Driefontein (thick filaments and rods). All the images were taken from a 45 mL borehole water sample. The scale bar represents 20 µm.